Mechanistic Analyses of Catalysis in Human Pancreatic α-Amylase: Detailed Kinetic and Structural Studies of Mutants of Three Conserved Carboxylic Acids†

Edwin H. Rydberg,‡ Chunmin Li,‡ Robert Maurus,‡ Christopher M. Overall,‡,§ Gary D. Brayer,‡ and Stephen G. Withers*,‡,||

Department of Biochemistry and Molecular Biology and Department of Oral Biological and Medical Sciences, University of British Columbia, Vancouver, British Columbia, Canada V6T 1Z3, and Department of Chemistry, University of British Columbia, Vancouver, British Columbia, Canada V6T 1Z1

Received September 20, 2001; Revised Manuscript Received January 9, 2002

ABSTRACT: The roles of three conserved active site carboxylic acids (D197, E233, and D300) in the catalytic mechanism of human pancreatic α-amylase (HPA) were studied by utilizing site-directed mutagenesis in combination with structural and kinetic analyses of the resultant enzymes. All three residues were mutated to both alanine and the respective amide, and a double alanine mutant (E233A/D300A) was also generated. Structural analyses demonstrated that there were no significant differences in global fold for the mutant enzymes. Kinetic analyses were performed on the mutants, utilizing a range of substrates. All results suggested that D197 was the nucleophile, as virtually all activity ($>10^5$-fold decrease in k_{cat} values) was lost for the enzymes mutated at this position when assayed with several substrates. The significantly greater second-order rate constant of E233 mutants on "activated" substrates (k_{cat}/K_m value for α-maltotriosyl fluoride = 15 s^{-1} mM^{-1}) compared with "unactivated" substrates (k_{cat}/K_m value for maltopentaose = 0.0030 s^{-1} mM^{-1}) strongly suggested that E233 is the general acid catalyst, as did the pH−activity profiles. Transglycosylation was favored over hydrolysis for the reactions of several of the enzymes mutated at D300. At the least, this suggests an overall impairment of the catalytic mechanism where the reaction then proceeds using the better acceptor (oligosaccharide instead of water). This may also suggest that D300 plays a crucial role in enzymic interactions with the nucleophilic water during the hydrolysis of the glycosidic bond.

α-Amylases [α(1−4)glucan 4-glucanohydrolase, EC 3.2.1.1] catalyze the hydrolysis of α(1−4) glycosidic linkages of starch and are widely distributed in nature. Nonarchaeal α-amylases are members of glycosyl hydrolase family 13 (*1*−*3*). Enzymes from this family perform a wide range of reactions that involve glycosidic bonds including hydrolysis, transglycosylation, cyclization, and disproportionation, and act on a range of substrates including those with α(1−4), α(1−6), or α(1,1) glycosidic bonds. Members of this family share a similar global polypeptide folding pattern, and exhibit strong sequence similarity in four small regions of their active sites.

Human pancreatic α-amylase (HPA) hydrolyzes α(1−4) glucosidic linkages with retention of configuration at the sugar anomeric center (*4*). Hydrolysis is thought to proceed via a double displacement reaction (Scheme 1) with general acid-catalyzed formation of a β-D-glycopyranosyl-enzyme intermediate followed by general base-catalyzed hydrolysis of this intermediate. HPA, as with the majority of retaining glycosidases, is believed to utilize active site carboxylic acids as the nucleophile and general acid/base catalysts in its hydrolytic reaction (*5*−*7*).

Rudimentary analyses of active site mutants from several family 13 α-amylases have demonstrated that the three completely conserved carboxylic acids D197, E233, and D300 (HPA numbering) are essential for efficient hydrolysis of oligosaccharides by these enzymes (*6*). Three-dimensional structural analyses of α-amylases from many species have confirmed that these three carboxylic acids are clustered at the bottom of a "V"-shaped active site cleft of a $(\beta/\alpha)_8$ barrel in the first domain of enzymes from this family (*8*−*16*). Although these residues are known to be important for catalysis and probable roles assigned, only in the case of the nucleophile mutant has the precise role in the catalytic mechanism been fully elucidated. This has been due, at least in part, to the difficulty of assaying mutants of these residues, since any activities of the mutants are essentially undetectable under standard assay conditions.

While relatively little detailed kinetic evidence exists upon which to base the assignment of the roles of the three catalytic carboxylic acids, a few notable structural analyses have provided valuable insights into the functions of these residues. The first evidence of a covalent glycosyl-enzyme intermediate was acquired in low-temperature ^{13}C NMR

† C.M.O. is funded by a Scientist Award from the Canadian Institutes for Health Research (CIHR). E.H.R. was supported by an MRC studentship. This project is funded by an operating grant from the Canadian Institutes for Health Research.

* Correspondence should be addressed to this author at the Department of Chemistry, University of British Columbia, Vancouver, British Columbia, Canada V6T 1Z1. Telephone: (604) 822-3402, Fax: (604) 822-8869, E-mail: withers@chem.ubc.ca.

‡ Department of Biochemistry and Molecular Biology.

§ Department of Oral Biological and Medical Sciences.

|| Department of Chemistry.

10.1021/bi011821z CCC: $22.00
Published on Web 03/07/2002

Scheme 1: Putative Mechanism of a Retaining α-Glycosidase

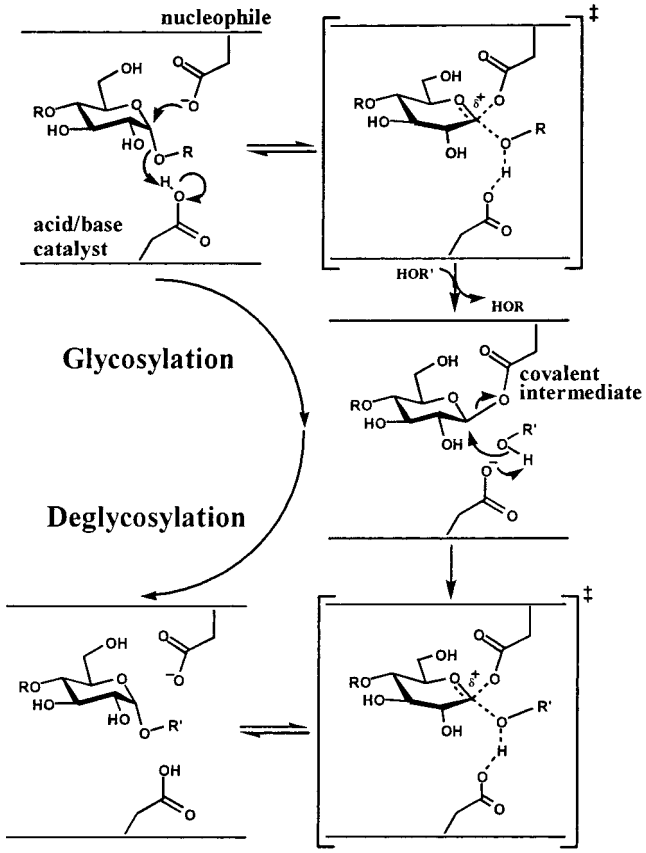

studies with porcine pancreatic α-amylase in 1989 (*17*). More recently, X-ray crystallographic studies on a family 13 cyclodextrin glucanotransferase (CGTase) mutant (E257Q) trapped as its glycosyl-enzyme intermediate via reaction with 4″-deoxymaltotriosyl fluoride demonstrated that D229 was the active site nucleophile, thus suggesting a similar role for the corresponding D197 of HPA (*18*). Similarly, structures of complexes with acarbose have substantiated this assignment of the nucleophile and allowed preliminary assignment of E233 as the acid/base catalyst (*8, 19*−*22*).

To probe the roles of the three active site carboxylic acids, D197, E233, and D300, in greater detail, we have generated the alanine and corresponding amide mutants of these residues and assayed these enzymes using both starch and "activated" α-glycosyl fluorides as substrates. Comparison of the kinetic parameters for hydrolysis of "natural" oligosaccharides with the parameters from hydrolysis of "activated" glycosyl fluorides along with studies of pH dependence and rescue of activity by exogenous anions provides valuable insights into the identity of the general acid/base catalyst as well as confirmation of the identity of the catalytic nucleophile.

MATERIALS AND METHODS

General Procedures. All buffer chemicals and other reagents were obtained from Sigma Chemical Co. unless otherwise noted. All chromatographic resins were purchased from Pharmacia. Synthesis of the substrate α-maltotriosyl fluoride (αG3F) has been described previously (*23*), as have the expression, purification, and deglycosylation conditions for the recombinant proteins (*24*). All oligodeoxyribonucleotides used in this study were synthesized on an Applied Biosystems PCR model 391 DNA synthesizer; the oligonucleotide sequences are given in Table 1. All sequencing was performed by the Nucleic Acids and Peptides Service (NAPS) at UBC.

Table 1: DNA Sequences of the Mutagenic Primers Used To Generate Mutants at Positions E233 and D300

mutagenic primer	sequence	mutants generated
wild-type sequence	C ATT TAC CAG GAG GTA ATT G	
AME233A	C ATT TAC CAG G**C**G GTA ATT G	E233A
AME233Q/K	C ATT TAC CAG **C**AG GTA ATT G	E233Q
wild-type sequence	GAT AAC CAT GAC AAT CAA C	
AMD300A	GAT AAC CAT G**C**C AAT CAA C	D300A
AMD300N	GGAT AAC CAT **A**AC AAT CAA C	D300N

Generation of Mutant α*-Amylases. (A) Generation of pHICL-AMY.* Digestion of the vector pHIL-S1 (Invitrogen, Inc.) with *Sac*I/*Sal*I gave a fragment of 2949 bp and the desired 5560 bp fragment which contained an F1 origin. The 5560 bp fragment was gel-purified in preparation for ligation with the fragment from pPIC9-AMY containing the HPA gene. The vector pPIC9-AMY was digested with *Sac*I, *Sal*I, *Sca*I, *Sph*I, and *Dra*III in 10% NEB Buffer 3 (New England Biologicals Inc.) at 37 °C overnight. The resulting 5040 bp fragment was easily gel-purified from the smaller DNA fragments of the other half of the vector, using a DNA gel-purification kit (Promega Inc.). Ligation of two of the gel-purified fragments (using the Rapid-Ligation kit from Promega Inc.) yielded the desired unique vector pHICL-AMY which contained both the F1 origin and the α-factor secretion sequence of the parent vectors.

(B) Mutagenesis. Generation of the D197A and D197N mutants was accomplished using a PCR methodology, as previously reported (*24*). Generation of the other mutant enzymes was achieved using Kunkel's method (*25*). To perform site-directed mutagenesis in *E. coli* by this method, the unique shuttle vector pHICL-AMY was utilized. Briefly, single-stranded dU-DNA was generated by the transformation of *E. coli* strain RZ1032 (dUT^-, UNG^-) with the pHICL-AMY vector, followed by infection with M13 filamentous phage (strain R408). Phage were precipitated from the bacterial supernatant, after centrifugation at 10000*g*, with 3.5% (w/v) poly(ethylene glycol) 8000, 0.4 M NaCl. After denaturation of the capsids by phenol/chloroform−isoamyl alcohol extraction, the phagemid DNA was ethanol-precipitated. Mutagenesis involved annealing the desired mutagenic primer (0.5 pmol) (Table 1) to the purified single-stranded dU-DNA in annealing buffer (10 mM $MgCl_2$, 1 mM DTT, 50 mM NaCl, 10 mM Tris-HCl, pH 8.0) at 55 °C for 5 min followed by slow-cooling to 22 °C. The extension reaction was performed by adjusting the buffer to 7.5 mM $MgCl_2$, 3 mM DTT, 38 mM Tris-HCl, pH 7.5, and incubating with Klenow fragment (1 unit), T_4 DNA ligase (1 unit), dNTPs (0.5 mM), and rATP (0.5 mM) for 2 h at 22 °C. Selection for the mutant strand was accomplished by the digestion of the dU-containing wild-type DNA after transformation into a dUT^+, UNG^+ *E. coli* strain (DH5α). Screening for successful mutations involved manual sequencing of the region of interest in the plasmids isolated from randomly selected colonies transformed with the cDNA

from the mutagenesis reaction mixture (*26*). A 60−80% mutation rate was commonly achieved. Mutant cDNAs were fully sequenced by the UBC NAPS unit automated sequencing service to confirm the fidelity of the reaction. Electroporation was then used to transform the *Pichia pastoris* strain GS-115 with the mutant cDNA (linearized with *Sac*I) following the Invitrogen protocol (Invitrogen, 1995).

(C) Screening for Successful Transformants. Transformed *P. pastoris* were screened following a standard protocol (Invitrogen, 1995), but with the addition of the "Yeastern" method (*27*). Briefly, screening involved patching the viable colonies from the transformation, grown on MD plates (minimal media containing dextrose), onto MM plates (minimal media containing MeOH) and, in the same pattern, onto fresh MD plates. After growing for 2 days at 30 °C, the plates were replica-plated, and the original MM plates were subjected to a yeastern as follows. These plates were covered with a wetted (soaked in MeOH for 5 min and water for 5 min) PVDF blotting membrane and several layers of paper towel (as in a nonelectrotransferred Western blot). These plates were then incubated at 30 °C for 3 h after which the membranes were developed by standard Western blotting methodology, with extra care taken during the washes to ensure the removal of any cells adhering to the membrane. Small BMGY cultures (10 mL) were then inoculated with the 10 colonies producing the darkest spots on the yeastern. These cultures were grown overnight at 30 °C before centrifuging (2000 rpm for 10 min). After decanting the supernatant, the pellets were resuspended in 2 mL of BMMY and induced overnight at 30 °C. After centrifuging (2000 rpm for 10 min), the supernatant was analyzed by SDS−PAGE and Western blot for the protein of interest.

(D) Expression in Pichia pastoris. Expression of the recombinant proteins was carried out as described in the Invitrogen Pichia Expression Manual for transformants of the MUT^s phenotype (Invitrogen Corp., 1995). Briefly, 8 × 500 mL of BMGY (1% yeast extract, 2% peptone, 1% yeast nitrogen base, 1% glycerol, 100 mM potassium phosphate, pH 6.0) cultures of *P. pastoris* was incubated at 30 °C for 1 day. After centrifugation (5 min, 5000*g*), the pellets were resuspended in 8 × 100 mL of BMMY medium (1% yeast extract, 2% peptone, 1% yeast nitrogen base, 0.5% MeOH, 100 mM potassium phosphate, pH 6.0), where expression was induced with MeOH. Following 2 days of expression at 30 °C with batchwise addition of 0.5% MeOH every 12 h, the *P. pastoris* cells were removed by centrifugation (10 min, 5000*g*), leaving the secreted α-amylase in the supernatant.

(E) Purification of Recombinant Enzymes. Purification of the recombinant enzymes was performed as previously described (*24*). The desired enzymes were obtained at greater than 99% purity upon elution from a phenyl Sepharose column followed by a Q Sepharose column. New column packings were used for all preparations of low activity mutants to minimize risk of cross-contamination with active enzyme. Treatment with endoglycosidase F prior to the Q Sepharose column, as described in (*24*), gave the homogeneous enzymes used in the further analyses.

Mass Determination. The mass determinations of the recombinant proteins were performed on a PE-Sciex API 300 triple quadrupole mass spectrometer (Sciex, Thornhill, Ontario, Canada) equipped with an Ionspray ion source (Table 2). Protein was loaded onto a C18 column (Reliasil, 1 × 150 mm) equilibrated with solvent A [solvent A: 0.05% trifluoroacetic acid (TFA), 2% acetonitrile in water] and eluted using a 1%/min gradient of solvent B (solvent B: 0.045% TFA, 80% acetonitrile in water) for 60 min, followed by 2 min of 100% solvent B. Solvent flow rates were constant at 50 μL/min.

Table 2: Mass Determinations for Wild-Type and Mutant α-Amylases Treated with Endoglycosidase F[a]

enzyme	theoretical mass (Da)	observed mass (Da)	difference
HPA	56091	56095	4
D197A	56047	56050	3
D197N	56089	56082	7
E233A	56033	56038	5
E233Q	56090	56069	21
D300A	56047	56042	5
D300N	56090	56085	5
E233A/D300A	55989	55992	3

[a] Theoretical masses are with the mass of one GlcNAc added to the protein mass. Error in measurement is 100 ppm (±6 Da). Unusual variation in masses (e.g., 56 076 − 56 090 for wt, 56 069 − 56 090 for E233Q) could be due to different forms of the N-terminal Gln as follows: theoretical masses (wt): nonglycosylated, 55 887; Wt with PYRR, 55 870; Wt+GlcNAc, 56 091; Wt +PYRR+GlcNAc, 56 074.

Table 3: Summary of Structure Determination Statistics

variant structures studied	D197A	E233A
Data Collection Parameters		
space group	$P2_12_12_1$	$P2_12_12_1$
unit cell dimensions (Å)		
a	52.88	52.92
b	69.52	74.72
c	131.60	136.94
total number of measurements	218502	234194
number of unique reflections	34783	40335
mean $I/\sigma I$[a]	14.6 (4.3)	19.6 (4.3)
multiplicity[a]	6.3 (3.5)	5.8 (3.1)
merging *R*-factor (%)[a]	6.9 (24)	5.0 (24)
maximum resolution (Å)	1.9	1.9
Structure Refinement Values		
number of reflections	33331	40110
resolution range (Å)	10−1.9	10−1.9
completeness within range (%)[a]	86.1 (82.9)	92.6 (80.9)
number of protein atoms	3943	3942
number of solvent atoms	138	119
average thermal factors (Å^2)		
protein atoms	19.04	22.74
solvent atoms	23.55	25.51
final *R*-factor/*R*-free (%)[b]	16.5/20.4	16.1/19.6
Structural Stereochemistry (rms Deviations)		
bonds (Å)	0.006	0.006
angles (deg)	1.298	1.308

[a] Values in parentheses refer to the highest resolution shell (1.97−1.90 Å). [b] For the *R*-free test, 10% of the data were kept aside.

Structure Determinations. Crystals of HPA mutant proteins were grown using conditions previously described (*22*). All crystallization and data collection procedures were conducted at room temperature. Diffraction data were collected on a Rigaku R-AXIS IIC imaging plate area detector system using Cu Kα radiation supplied by a Rigaku RU300 rotating anode generator operating at 50 kV and 100 mA. Intensity data were integrated, scaled, and reduced to structure factor amplitudes with the HKL suite of programs (*28*). Data collection statistics are provided in Table 3. The results of diffraction data collections showed that the mutant crystals obtained were of two types. This phenomenon has been noted

before in this system and appears to be linked to the extent of glycosylation at a site remote from the active site (*22*). For the first crystal type, comprising crystals of D197A, unit cell parameters were found to be isomorphous with those of wild-type HPA. In this case, the starting structural refinement model used was that of the wild-type protein with D197 substituted with alanine. The second crystal form, found for E233A crystals, was isomorphous with that previously described for crystals of a D300N/acarbose complex (*22*). Therefore, the structure of this latter complex was used as the starting refinement model in this case, with an aspartate substituted for N300, the acarbose atoms deleted, and E233 represented as an alanine.

Refinement of both structural models was accomplished with CNS (*29*). In these analyses, cycles of simulated annealing, positional, and thermal *B* refinements were alternated with manual model rebuilding with O (*30*). The complete polypeptide chain for both refinement models was examined periodically during this process with F_o-F_c, $2F_o-F_c$, and fragment-deleted difference electron density maps. During such examinations, the positions of solvent molecule peaks were assigned, and their validity was assessed based on both the hydrogen bonding potential to protein atoms and the refinement of a thermal factor of <75 Å^2. An *N*-acetylglucosamine moiety was found bound to the side chain of N461 only in the structure of the D197A mutant, and was refined accordingly. Final refinement statistics for each structure determination are detailed in Table 3. Coordinate error, as estimated from a Luzzati plot (*31*), is 0.20 Å for both the D197A and E233A HPA mutants.

Kinetic Analyses. (A) General Procedures. Fluoride ion concentration was measured using an Orion 96-09 combination fluoride ion selective electrode coupled to an Accumet 925 pH/ion meter (Fischer Scientific). The ion meter was interfaced with a Pentium 133 MHz personal computer for data collection. Alternatively, the electrode was fitted to a signal amplifier box connected to a personal computer, and data were collected using Logger Pro (Vernier Software Inc). Assays measuring the sugar products were performed using a Waters HPLC (model 501 pump, single-port manual injector) instrument with a refractive index detector (model 410). Reaction products were separated using a Waters Dextropak 8/10 radial compression column with a Resolve C-18 guard column run in a deionized H_2O mobile phase at a 1.0 mL/min flow rate. The data were collected, and peak areas calculated, using the Baseline 810 software. Where product concentrations were desired, the peak areas were compared to those measured from a standard curve. For all kinetic assays, the data were fit to the desired model using the nonlinear regression program GraFit 4.0 (Erithacus Software Inc., Staines, U.K.). The error values noted in the data tables refer to the error in fitting the data to the model.

(B) Measuring Specific Activities Using the Dinitrosalicylic Acid (DNS) Assay. Specific activities of crude (supernatant) and purified recombinant enzymes were measured using the dinitrosalicylic acid assay (*32*). An enzyme sample, either from culture supernatant or purified (up to 500 μL), was added to a solution of soluble starch (500 μL, 1 g/L) and incubated at 30 °C in 20 mM potassium phosphate buffer, pH 6.9, containing 25 mM NaCl. For *p*HPA, the incubation time was 3 min. The mutant enzymes were incubated for between 8 and 24 h. The reactions were stopped by addition of 1.0 mL of the DNS solution (10 mg/mL 3,5-dinitrosalicylic acid and 30 mg/mL Na,K-tartrate in 0.4 M NaOH). Color was developed by boiling the stopped samples for 5 min, followed by cooling with cold tap water and dilution with 10.0 mL of distilled water. The samples were then measured spectrophotometrically at 546 nm. Concentrations of sugar reducing ends were calculated by comparison to a maltose standard curve.

(C) Standard Assay for Measuring Hydrolysis of Maltooligosaccharyl Fluorides. The kinetic parameters k_{cat} and K_m for the recombinant proteins were determined by monitoring the release of fluoride from αG3F and α-maltosyl fluoride (αG2F) as described previously (*33*). The assays were performed at 30 °C in 20 mM sodium phosphate buffer, pH 6.9, containing 25 mM NaCl. Stock enzyme (5 μL of 50 nM wild-type enzyme, or 50 μL of 18 μM mutant enzyme) was added to glass cells containing various concentrations of substrate in a total assay volume of 300 μL. For each Michaelis−Menten curve generated, initial rates for 6−8 substrate concentrations were used. Concentrations of αG3F were typically varied between 50 μM and 5 mM, while the range of αG2F concentration was generally from 500 μM to 20 mM. The initial rates were determined from the first 5 min of data. Controls were performed to compensate for the spontaneous hydrolysis of the substrates.

(D) pH Stability. The pH stabilities of the recombinant proteins were studied using the standard glycosyl fluoride assay performed at 13 different pH values, from 4.0 to 10.0 in increments of 0.5 pH unit. Only one concentration of αG3F (2 mM) was assayed at each pH. Assay solutions (total volume 300 μL) were buffered with 180 μL of a solution of 100 mM potassium phosphate and 100 mM sodium citrate containing 25 mM NaCl and 500 μM calcium chloride.

(E) Determining pH Dependence of k_{cat}/K_m (Substrate Depletion Method). The pH dependence of the second-order rate constant k_{cat}/K_m was studied using the substrate depletion method. Measurements of fluoride release from αG3F were followed at 13 different pH values, from 4.0 to 10.0 in increments of 0.5 pH unit. Assay solutions (total volume 300 μL) were buffered with 180 μL of a solution of 100 mM potassium phosphate and 100 mM sodium citrate containing 25 mM NaCl and 500 μM calcium chloride. At each pH value, the release of fluoride resulting from the reaction of enzyme with αG3F at concentrations ($<1/5$)K_m was followed as a function of time for a minimum of 3 half-lives. Enzyme concentration was chosen so that, where possible, $t_{1/2}$ was equal to approximately 15 min. The resulting data were then fit to a first-order product accumulation model using GraFit version 4.06 (Erithacus Software Inc., Staines, U.K.). The pseudo-first-order rate constant for the curve (V_{max}/K_m) was divided by the enzyme concentration (E_o) to give the k_{cat}/K_m value.

(F) Determining pH Dependence of k_{cat}. Determination of the pH dependence of k_{cat} for the recombinant proteins was achieved using the standard glycosyl fluoride assay. However, measurements of fluoride release from αG3F were followed at 13 different pH values, from 4.0 to 10.0, in increments of 0.5 pH unit. For each enzyme, the substrate (αG3F) was assayed at a concentration that gave a rate equal to V_{max}, typically in the range 2−5 mM. Assay solutions (total volume 300 μL) were buffered with 200 μL of a solution of 100 mM potassium phosphate and 100 mM sodium citrate

containing 25 mM NaCl. Calcium chloride was also added to the assay mixture to a concentration of 500 μM.

(G) Determination of Kinetic Parameters with Maltopentaose. An HPLC stopped-assay was used to determine the kinetic parameters of the wild-type and mutant enzymes with maltopentaose. Assay solutions (200 μL total volume) were buffered with 10 mM potassium phosphate and 20 mM NaCl at the pH optimum for each enzyme. Enzymes were assayed at seven substrate concentrations (0.1−3.0 mM) of G5. Assays were incubated at 30 °C, and 25 μL aliquots were taken at four time points for each concentration. The reactions were stopped by direct injection of the mixture into the HPLC through a Waters Resolve-C18 guard column. Total incubation time for the wild-type reaction (2.5 nM enzyme) was 1 h, for E233Q (0.7 μM) 50 h, and for D300N (1.3 μM) 10 h. Product concentrations were determined by the relative refractive index (reference cell was purged for 30 min with mobile phase prior to measurements) after separation from substrates by HPLC using a Waters Dextropak 8/10 radial compression column with a Resolve C-18 guard column. The H_2O mobile phase was run at a flow rate of 1.0 mL/min, and retention times were the following: G2, 2.8 min; G3, 3.7 min; G5, 5.8 min. A standard curve was constructed using maltopentaose concentrations of 0.1, 1.0, and 10.0 mM, each measured in triplicate, and used to determine the substrate concentration at each time point.

(H) Product Distribution Studies. Product distributions were determined by following a procedure similar to that used in the kinetic analyses of G5 hydrolysis. Substrate concentrations (αG3F and G5) of 5 and 20 mM each were treated with enzyme, and the products formed were determined at regular intervals until the substrate was fully hydrolyzed, or for a period of 5 days, whichever occurred first.

(I) Azide Rescue of Alanine Mutants. αG3F (30 μL, 20 mM) was added to solutions of sodium azide (200 mM to 5.0 M) in buffer (250 μL, 100 mM potassium phosphate, 10 mM NaCl, pH 6.0) in a 1 mL flat-bottomed glass vial. The solution was incubated, with the fluoride electrode, at 30 °C for 5 min before measuring the rate of spontaneous hydrolysis for 5 min. Enzyme (20 μL of 120 μM D197A, 30 μL of 710 nM E233Q, or 10 μL of 38 μM D300A) was then added. After mixing, the rate of fluoride release was followed for 10 min, or for less than 10% hydrolysis. After correcting for spontaneous hydrolysis, the data were successfully fit to the Michaelis−Menten model in all cases, although inhibition was observed at high azide concentrations (greater than 2 M) for E233A and D300A.

RESULTS AND DISCUSSION

Cloning. The unique shuttle vector pHICL-AMY (where AMY refers to the human pancreatic α-amylase gene) was generated in order to perform site-directed mutagenesis in *E. coli* by the method of Kunkel (*25*). This was achieved by combining a vector which contained an F1 origin (pHIL-S1) with one containing the α-factor secretion sequence (pPIC9), which is thought to be more efficient than the PHO1 secretion sequence (pHIL-S1) (*34*).

Upon digestion with *Sac*I/*Sal*I, the vector pHIL-S1 produced two fragments of 2949 and 5560 bp, which could be readily purified. However, after *Sac*I/*Sal*I digestion, the pPIC9-AMY vector gave fragments of 5040 and 4490 bp, which could not be satisfactorily resolved by agarose gel electrophoresis under the desired conditions. The digestion of pPIC9-AMY was therefore carried out with *Sca*I, *Sph*I, and *Dra*III in addition to *Sac*I and *Sal*I in order to further digest the unwanted fragment, thus leaving a trivial gel purification of the fragment containing the AMY insert. Ligation of the 5.6 kbp fragment of pHIL-S1 and the 4.5 kbp fragment of pPIC9-AMY yielded the unique vector pHICL-AMY which contained both the F1 origin and the α-factor secretion sequence of the parent vectors.

Table 4: Specific Activities of Recombinant α-Amylases on Soluble Potato Starch

protein	specific activity on soluble starch (units/mg of protein)[a]	protein	specific activity on soluble starch (units/mg of protein)[a]
HPA	5.5×10^3		
D197A	none detected	D300A	0.010
D197N	none detected	D300N	0.020
E233A	0.280	E233A/D300A	0.050
E233Q	0.020		

[a] Using soluble starch as a substrate, 1 unit releases 1 μmol of reducing groups (calculated as maltose) per minute at 30 °C, pH 6.

Determination of Kinetic Parameters. Although crude assays of specific activity of the recombinant enzymes were performed using the DNS method, and HPLC was utilized to assay maltopentaose degradation, the predominant method of assaying the recombinant enyzmes was through the use of α-glycosyl fluorides. Kinetic parameters for the recombinant enzymes were determined in a continuous assay by measuring the rate of release of fluoride ion from α-maltosyl fluoride (αG2F) and α-maltotriosyl fluoride (αG3F) using a fluoride-selective electrode. This assay method has been successfully utilized previously for measuring wild-type α-amylase activity (*4*, *22*, *24*), and is one of the few convenient, continuous, noncoupled assays for α-amylases.

Early studies of the reactions of αG2F with α-amylases suggested that the predominant mechanism of fluoride release was through transglycosylation (*35*). These experiments, however, were performed at high αG2F concentrations (typically greater than 20 mM, $K_m = 3.0$ mM) with product determination occurring after 20−30 min. Consequently, these studies were reporting conditions that may not be typical of the initial reaction (that is, during measurement of v_o). In our studies, wild-type α-amylase showed little evidence of transglycosylation using αG2F or αG3F as substrate under standard assay conditions (substrate concentrations less than 7 times the K_m value, and the reaction measured over 5 min) by either TLC (data not shown) or HPLC (discussed below), although transglycosylation products were observed after periods of extended incubation.

(A) Starch. The culture supernatant and purified forms of all recombinant proteins were assayed by the DNS (dinitrosalicylic acid) method as a rapid assay of specific activity on the natural substrate. No activity was detected in the supernatants under standard DNS assay conditions for any of the mutant proteins (data not shown), and the specific activity in the purified form (Table 4) could only be determined after extended incubation (typically at 12−24 h). As only approximate specific activities were deemed neces-

sary, and because large amounts of enzyme were required for each assay (except for the wild-type), only a single assay was performed for each enzyme during the extended incubation. Therefore, the specific activities of the mutant enzymes represent only crude estimates.

From Table 4, it appears obvious that all the mutations generated resulted in enzymes with significantly reduced ability to hydrolyze starch, as their specific activities are at least 10^4-fold less than that of the wild-type enzyme. These results are essentially the same as those from previously reported starch assays for enzymes mutated at any one of the three active site carboxylic acids [reviewed in (*6*, *7*)].

(B) α*-Glycosyl Fluorides (*α*G2F,* α*G3F).* Upon successful purification of recombinant HPA from *Pichia*, initial kinetic characterization necessarily focused on ensuring that there were no gross differences between the recombinant wild-type (rHPA) and the native (pancreas-derived, HPA_{wt}) enzymes. Kinetic parameters (Table 5) for rHPA (αG3F: $k_{cat} = 280\ s^{-1}$, $K_m = 0.3$ mM) compared favorably with those of the pancreas-derived enzyme [αG3F: $k_{cat} = 250\ s^{-1}$, $K_m = 0.5$ mM (*22*, *24*)], suggesting that the cloning and expression had been successful. In addition, the differential glycosylation of rHPA and the native enzyme did not seem to influence the kinetic parameters since they did not change significantly for rHPA upon deglycosylation with endoglycosidase F. This demonstrated that glycosylation on the *C*-domain, even with a large, 13-residue glycosyl group, did not influence the catalytic properties of the distant active site with either small or large substrates (Tables 4 and 5).

Following the confirmation that rHPA had similar kinetic parameters to the native HPA, the mutant α-amylases were kinetically characterized. Although no significant activity had been observed for enzymes in which any of the three active site carboxylic acids (D197, E233, D300) were replaced when assayed with starch [reviewed in (*6*, *7*), and Table 4], the kinetic parameters in Table 5 clearly demonstrate that differences in activity between the various mutants can be observed using α-glycosyl fluoride substrates. It is also obvious that most of the mutants show dramatic decreases in their specificity constants (k_{cat}/K_m) when compared with the wild-type enzyme. Although the K_m values for the mutants only differ from wild-type by at most an order of magnitude, the k_{cat} values vary over 6 orders of magnitude. Consequently, the specificity constants for the recombinant enzymes vary by 7 orders of magnitude.

Determining the Validity of the Low Enzyme Rates. A question that plagues any detailed analyses of low-activity enzyme mutants is whether the observed activity is due to the mutant itself or whether it results from contaminating wild-type enzyme. This is a concern for any mutant, and especially for amide mutants of carboxyl groups, as these could be deamidated during expression, purification, or storage, thereby regenerating some wild-type enzyme (*36*). The results of several experiments suggest that there is no significant contamination by wild-type HPA in the low-activity (specifically D197A, and D197N) enzyme preparations. Indeed, based upon the activity measured at the enzyme concentrations and reaction times employed for these mutants, the maximum amount of contaminating wild-type enzyme would be less than 0.00000005% of the total protein. Importantly, the K_m values measured for D197A and D197N with the αG3F substrate were 10-fold and 3-fold, respectively, greater than the K_m value of *p*HPA, suggesting that, since the K_m value for a substrate is a property intrinsic to a given enzyme, the activity measured is not due to the wild-type enzyme, but is a true activity of the mutants. Comparable differences in K_m values were also seen for the other mutants.

Structural Integrity of Amylase Mutants. The structural integrity of the recombinant amylase mutants was studied by two means. The small error between predicted and observed mass, as determined by ESI-MS (Table 2), was suggestive of the properly sized polypeptide chains being expressed. Interestingly, the mass determined for freshly prepared mutants was lower by approximately 17 Da than the mass determined at a later date. This is ascribed to the production of the protein with its N-terminal glutamine in the form of a cyclic pyroglutamate residue, which hydrolyzes with time. X-ray structures in all cases showed the pyroglutamate form, consistent with crystallizations being performed on very fresh samples (*14*). Theoretical masses presented in Table 2 represent the "aged" hydrolyzed form since the mass spectra were collected at a later date, when the kinetic studies were performed. In only one case, E233Q, was the difference between theoretical and observed mass greater than 7 Da, the mass being consistent with the pyroglutamate form. For some reason, in that case, hydrolysis of the pyroglutamate seems to be slower. X-ray crystallographic studies were also used to confirm the integrity of the active site for D197A and E233A (Figure 1). For D197A,

Table 5: Kinetic Parameters for Recombinant HPA's with α-Maltotriosyl Fluoride and α-Maltosyl Fluoride[a]

	kinetics (αG3F)				kinetics (αG2F)			
enzyme	k_{cat} (s^{-1})	K_m (mM)	k_{cat}/K_m ($s^{-1}\,mM^{-1}$)	*x*-fold decrease in k_{cat}/K_m	k_{cat} (s^{-1})	K_m (mM)	k_{cat}/K_m ($s^{-1}\,mM^{-1}$)	*x*-fold decrease in k_{cat}/K_m
HPA_{wt}	(283)	(0.51)	(555)		443	4.5	98	
$rHPA_{gly}$	280	0.34	830	1.0	150	2.1	73	1.0
$rHPA_{degly}$	215	0.26	850	0.98	130	1.8	75	1.0
D197A	1.0×10^{-4}	3.8	2.6×10^{-4}	3.1×10^7	N/A	N/A	N/A	N/A
D197N	7.3×10^{-4}	1.1	6.7×10^{-4}	8.1×10^7	N/A	N/A	N/A	N/A
E233A	0.82	1.1	0.75	1.1×10^3	N/A	N/A	N/A	N/A
E233Q	0.51	0.033	15	8.3×10^2	0.10	0.10	0.99	74
D300A	0.010	0.47	0.021	4.0×10^4	0.016	6.2	0.0026	2.8×10^4
D300N	0.15	0.89	0.17	4.9×10^3	0.18	4.8	0.038	1.9×10^3
E233A/D300A	0.0027	0.79	0.0034	2.4×10^5	0.021	29.0	0.00074	9.9×10^4

[a] All assays were performed at pH 7.0. All kinetic parameters in this table were determined at pH 7.0. HPA_{wt} = HPA isolated from human pancreas; $rHPA_{gly}$ = heterogeneously glycosylated HPA expressed from *Pichia pastoris*; $rHPA_{degly}$ = endoglycosidase F treated HPA, expressed from *Pichia pastoris*; N/A = data not acquired. Average errors in kinetic parameters: K_m (±7−10%) and k_{cat} (±5−7%).

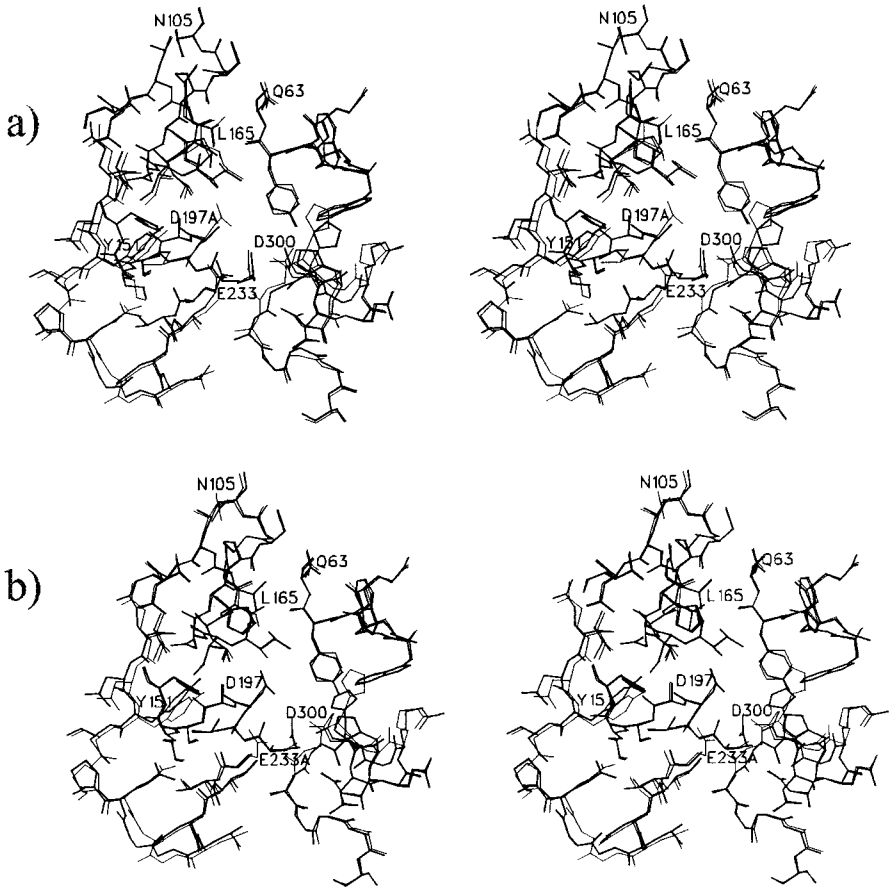

FIGURE 1: Stereo plots of the active site region in the (a) D197A and (b) E233A mutant structures of human pancreatic α-amylase (thick lines). To facilitate comparisons, the structure of wild-type HPA (thin lines) has been overlaid on these drawings. The three catalytic residues D197, E233, and D300 have also been labeled to clearly indicate their relative positioning within the active site region.

no significant perturbations of the polypeptide chain were observed around residue 197, although there was a small reorientation in the side chain of D300. This reorientation is likely due to the small reorientation of residues 303−307, which are part of a flexible surface loop in the vicinity of the substrate binding cleft. In the structure of E233A, there is also no significant perturbation of the backbone around the mutated residue. However, once again there is a small shift in residues 305−310 of the flexible surface loop near the substrate binding cleft. Taken together, these data suggest no significant alterations in either the global fold or the active site integrity of the amylase mutants, apart from those that were desired.

Dependence of k_{cat} and k_{cat}/K_m on pH. The pH dependence of the first-order (k_{cat}) and second-order (k_{cat}/K_m) rate constants for the enzymatic reactions was investigated for several recombinant enzymes. The k_{cat}/K_m value for cleavage of αG3F at each pH was determined by the substrate depletion method, where k_{cat}/K_m is the pseudo-first-order rate constant for the reaction at substrate concentrations lower than 20% of the K_m value. The k_{cat} values were studied by assaying with substrate concentrations at which the enzyme-catalyzed hydrolysis was at V_{max}. Full Michaelis−Menten curves were generated at the low and higher pH values to ensure that the K_m value did not change appreciably with pH.

The pH dependence of k_{cat} for hydrolysis of αG3F by wild-type HPA was similar to that reported in the literature for

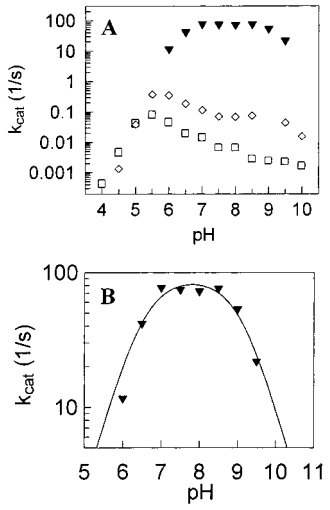

FIGURE 2: pH dependence of k_{cat} for hydrolysis of αG3F by wild-type HPA (▼), D300A (□), and D300N (◇) (A). Data for HPA-wt shown expanded (B). pH optima for all mutants are shifted 1.2 pH units more acidic than for *p*HPA.

hydrolysis of the PNP-maltoside (*37*) with $pK_{a1} = 6.5$ and $pK_{a2} = 9.0$ and a pH optimum from 7.0 to 8.5. However, the pH profiles for both D300N and, to a lesser extent, D300A revealed a dependence of k_{cat} values on the ionization states of three residues (Figure 2) with pK_a values of $pK_{a1} = 5.5$, $pK_{a2} = 6.3$, $pK_{a3} = 9.0$ in each case. Similar behavior was seen in the pH dependence of the k_{cat}/K_m values for these mutants (Figure 3).

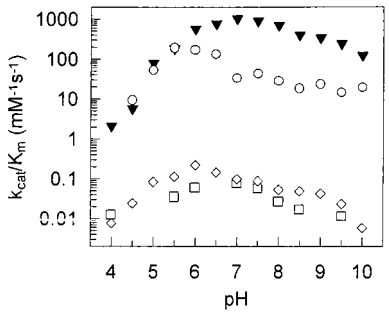

FIGURE 3: pH dependence of k_{cat}/K_m for hydrolysis of αG3F by wild-type HPA (▼), E233Q (○), D300A (□), and D300N (◇). pH optima for all mutants are shifted 0.5−1.2 pH units more acidic than for *p*HPA. The acidic pK_a values for the mutants were the same, shifted 1 pH unit lower than wild-type HPA, while pK_a values of the basic limbs decreased by up to 2 pH units from the wild-type enzyme.

Product Distribution Studies. Determination of the products of the reactions, particularly with the mutant enzymes, is necessary to fully understand the mechanism of HPA. It is important to determine whether kinetic assays are measuring hydrolysis or transglycosylation, and whether mutation of an active site residue has resulted in a change of this mechanism.

Product distributions were determined by HPLC for the reactions of wild-type HPA, E233Q, and D300N with both αG3F and G5. The substrates were assayed at concentrations of 5 mM since this was a standard assay concentration that gave maximal rates for all enzymes while still resulting in a strong response from the refractive index detector. Higher substrate concentrations were not necessarily representative of the assay conditions in previous studies, while lower concentrations were difficult to detect. The reactions were followed until the substrate was depleted or for 20 h, whichever occurred first.

(A) α*-Maltotriosyl Fluoride.* The reactions of the three recombinant enzymes with αG3F resulted in similar initial products, which then varied dramatically as the reaction progressed. Early stages of reaction (first 5 min) in each case involved hydrolysis of αG3F accompanied by the formation of small amounts of G4 and G6, presumably by transglycosylation. The reaction catalyzed by wild-type HPA was complete after the first hour, and the principal products were G3 and G2 (Figure 4). In addition, the two anomers of G4 can be observed (retention times = 5.3 and 6.3 min) after 5 min of the reaction, as can a small peak (retention time = 13.1 min) corresponding to G6F. Maltotriose (retention time = 4.4 min) appears to be produced from the hydrolysis of αG3F and possibly from hydrolysis of G6F while, due to the absence of a peak corresponding to glucose (retention time = 3.4 min), all of the G2 (retention time = 3.9 min) must arise ultimately from hydrolysis of G6F by way of G4.

An interesting observation regarding the time-course of hydrolysis of αG3F by E233Q is the apparent inhibition of this mutant enzyme early in the reaction. From the progress curves (data not shown), it was clear that the E233Q-catalyzed hydrolysis of αG3F proceeds very rapidly for the first 5 min, after which the hydrolysis reaction appears to virtually cease. Since early studies demonstrated that E233Q was stable at 30 °C for several days, and there still appears to be a significant amount of substrate remaining, this effect would appear to be due to the inhibition of the enzyme,

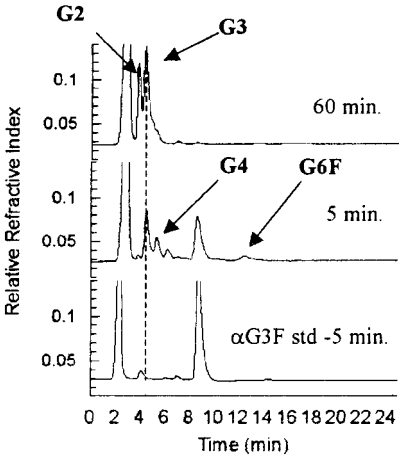

FIGURE 4: Product analysis of the reactions of wild-type HPA with αG3F. The reaction initially proceeds by hydrolysis with small amounts of transglycosylation products being observed after 5−10 min. The final products are G3 and G2 (the latter is presumably produced from hydrolysis of transglycosylation products).

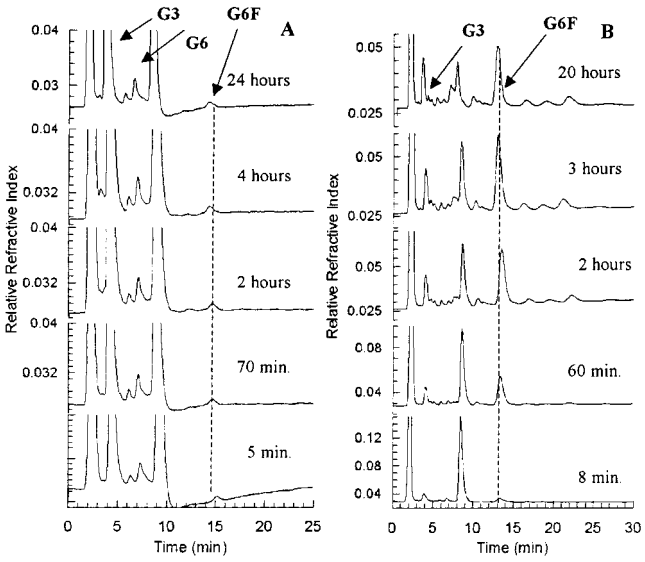

FIGURE 5: Product analysis of the reactions of E233Q (A) and D300N (B) with αG3F. Although the reaction of E233Q proceeds predominantly by hydrolysis, note that it appears to be inhibited after about 5 min. This is possibly due to formation of a small amount of transglycosylation product (retention time = 15 min) that functions as a good inhibitor. In contrast, the reaction of D300N with αG3F seems to proceed by both hydrolysis and transglycosylation, with transglycosylation becoming dominant after about 20 min.

perhaps by a transglycosylation product. The observation, by both TLC (not shown) and HPLC, of small amounts of a longer oligosaccharide produced in the reaction (Figure 5) may support this. Indeed, G5 and G6 were tested as inhibitors of both E233Q and D300N (which was used as a control, since similar inhibition has not been previously observed with this enzyme). Maltopentaose and maltohexaose were found to inhibit E233Q with K_i values of 3 and 10 μM, respectively (data not shown), while the K_i value for G5 against D300N was 0.5 mM. Maltotriose did not inhibit either enzyme appreciably, even at concentrations up to 1 mM.

The products of the reaction between D300N and αG3F (Figure 5B) are more numerous than with either of the other recombinant enzymes tested. The initial reaction appears to proceed almost equally via hydrolysis and transglycosylation,

Table 6: Kinetic Parameters for the Reactions of *p*HPA, D197N, E233Q, and D300N with αG3F and G5, and Specific Activities on Soluble Starch[a]

enzyme	k_{cat} (s^{-1})	K_m (mM)	k_{cat}/K_m (s^{-1} mM^{-1})	U (mmol min^{-1} mg^{-1})	*x*-fold decrease in k_{cat}/K_m or U compared to wild-type
*p*HPA					
αG3F	215	0.26	850		
G5	95	0.70	136		
starch				5.5×10^3	
D197N					
αG3F	7.3×10^{-4}	1.1	6.7×10^{-4}		1.3×10^6
G5		NR			–
starch				NR	–
E233Q					
αG3F	0.51	0.033	15		5.7×10^1
G5	0.011	0.3	0.0030		2.2×10^4
starch				0.020	2.8×10^5
D300N	0.15	0.89	0.17		5.0×10^3
αG3F	0.083	2.3	0.037		1.8×10^3
G5				0.020	2.8×10^5
starch					

[a] Average errors in kinetic parameters: K_m (±7−10%) and k_{cat} (±5−7%). NR: No reaction.

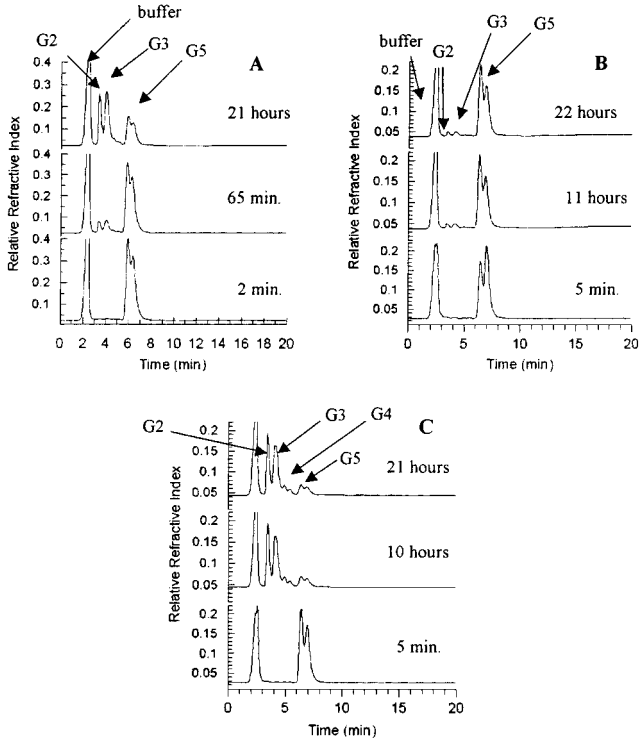

FIGURE 6: Product analysis of the reactions of wild-type HPA (A), E233Q (B), and D300N (C) with maltopentaose. Wild-type HPA and E233Q appear to generate the hydrolysis products G2 and G3. However, although G2 and G3 are the major products for D300N, small amounts of G4 are also detected.

as products from both reactions (G3 from hydrolysis, and G6F from transglycosylation) are detected after 5 min. Although G3 could be produced from either the hydrolysis of αG3F or the hydrolysis of G6F, the kinetic parameters listed in Table 6 suggest that the former proceeds at a greater rate. Perhaps the most interesting feature of the reaction of D300N with αG3F is the wide variety of transglycosylation products generated and, specifically, the large amount of G6F produced in the first hour. Apparently, the D300N mutation disrupts the deglycosylation step of the mechanism in such

Scheme 2: Schematic Representations of the "Standard" Hydrolysis of G5 (A) and the Possible Transglycosylation Pathway Utilized by D300N To Generate G4 (B)

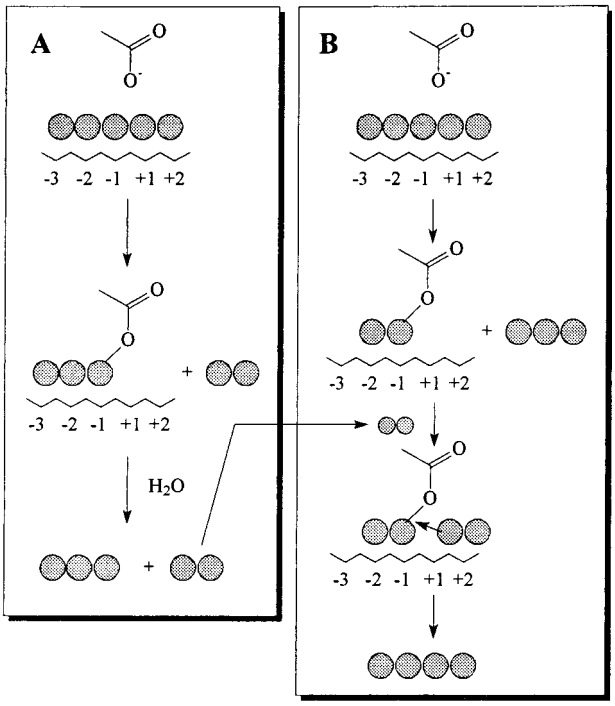

a way that oligosaccharides are favored over water as acceptors.

(B) Maltopentaose. Analyses of the products formed at different times during the reactions of wild-type HPA, E233Q, and D300N (Figure 6) with maltopentaose suggest that all three of these enzymes cleave G5 in a similar manner. In the reactions with wild-type HPA and E233Q, the only products appear to be G2 and G3. For the native HPA, these products have previously been shown to arise from a single productive G5 binding mode resulting in G2 as the aglycone (*22*) (Scheme 2). The reaction of D300N with G5 also produces predominantly G2 and G3, though G4 is also observed as a product (Figure 6C). Since no glucose is apparently produced, it is difficult to hypothesize how the G4 was generated. One possibility might be that D300N hydrolyzes G5 in two productive binding modes wherein either G2 or G3 is the aglycone. If deglycosylation of the maltosyl−enzyme complex was slower with water than with an oligosaccharide acceptor, then either G4 (G2 donor, G2 acceptor) or the substrate G5 (G2 donor, G3 acceptor) would be produced. Due to the relatively small amount of G4 produced, it is likely that the most favorable productive binding mode is with G2 as the aglycone, as in the wild-type enzyme. If this were not the case, then either the proportion of G4 produced should be much greater, or the enzyme would appear inactive as it would continuously cycle product back into substrate.

Evidence for D197 Acting as the Catalytic Nucleophile. The catalytic nucleophile is arguably the single most important amino acid residue in the active site of HPA. Based upon previous experience with β-glycosidases in particular, mutation of the enzymic nucleophile to a more chemically inert residue such as alanine or asparagine should essentially abolish all enzymatic activity (*38*). Indeed, mutants of the putative nucleophile D197 had the lowest k_{cat}/K_m values of

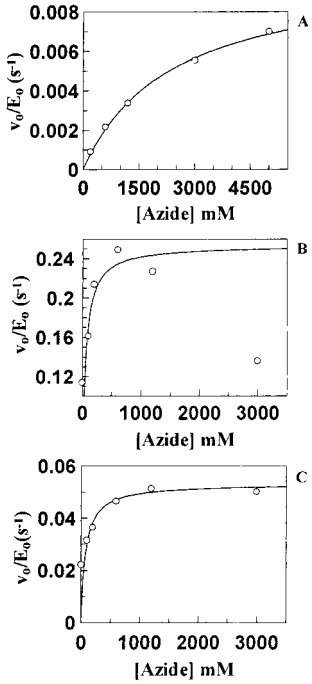

FIGURE 7: Azide rescue of mutant enzyme activities using αG3F as substrate. D197A (A) experiences a 10-fold increase in activity in the presence of >4 M NaN_3, while 1 M azide results in 2-fold and 8-fold increases in the activities of E233A (B) and D300A (C), respectively. E233A and D300A are inhibited by azide concentrations above 1 M.

all the recombinant enzymes, the second-order rate constant being 6 orders of magnitude lower than that of wild-type enzyme. Since the K_m values are increased by only 3 and 10 times (D197N and D197A, respectively), and no significant structural changes have been observed (Figure 1), the drastic reduction in specificity constant clearly results from severe impairment of the chemical steps. This is precisely what would be expected for enzymes lacking the catalytic nucleophile. In contrast, similar mutations to E233 and D300 yield mutant enzymes that cleave substrates at rates that are several orders of magnitude greater than those of the D197 mutants. Indeed, even the double mutant E233A/D300A has a k_{cat} value that is greater than that of the D197 mutants.

Creation of the alanine mutant should leave a "hole" in the active site that could be filled by small nucleophiles, thus permitting a chemical rescue of enzyme activity, generating a product of inverted anomeric stereochemistry. Such a mutant should therefore generate a stable β-glycosyl azide in this case. The rate enhancement for D197A with sodium azide (Figure 7A) was the largest observed for any of the mutants tested (10-fold, compared with 2-fold for E233A and 8-fold for D300A; Figure 7B,C, respectively). This effect is consistent with D197 being the nucleophile in a double displacement reaction. Unfortunately, no glycosyl azide product was observed by ^{1}H NMR although several different reaction conditions were tried. It therefore appears that the accelerated reaction is still too slow to generate sufficient products to be observed by NMR. Alternatively, any β-glycosyl azide product formed, as expected in the reaction with D197A, may itself act as a substrate, as has been seen in the equivalent reaction with β-glycosidases (*39*).

Evidence for E233 Acting as the General Acid/Base Catalyst. The general acid catalyst acts during the glycosylation step of the double displacement reaction to protonate the leaving group of natural substrates such as maltopentaose. In contrast, departure of the leaving group from "activated" substrates such as α-glycosyl fluorides does not require the assistance of a general acid catalyst. Thus, for enzymes in which the general acid catalyst has been mutated, a much larger decrease in k_{cat}/K_m value (which reflects the glycosylation step) should be observed with maltopentaose as substrate than with αG3F. In addition, mutation of the general acid catalyst to alanine should permit chemical rescue of the activity by a small nucleophile such as azide attacking the glycosyl-enzyme intermediate. The product of such a reaction should be the α-glycosyl azide.

From Table 6 it is apparent that mutation of E233 results in the most disproportionate change in k_{cat}/K_m values for hydrolysis of αG3F versus G5 when compared to the wild-type enzyme (57-fold decrease and 2.2×10^4-fold decrease, respectively). This suggests that E233Q contains enough catalytic machinery to hydrolyze αG3F relatively efficiently, but is missing a crucial component for hydrolysis of G5. A key difference between these two substrates is in their need for general acid catalysis. Therefore, comparison of second-order rate constants for hydrolysis of an "activated" and a natural substrate strongly favors the conclusion that E233 is the general acid catalyst.

The small rate enhancement (2.2-fold) for E233A with sodium azide (Figure 7B) when assayed with α-glycosyl fluoride substrates is far less than that generally observed with β-glycosidases ($10-10^4$-fold) (*40*−*42*), but is completely consistent with the rate enhancement observed for the CGTase acid/base catalyst mutant E257A (1.8-fold) with sodium azide (*43*). Unfortunately, no glycosyl azide product was observed by ^{1}H NMR although several different reaction conditions were attempted. It is probable that the accelerated reaction is still too slow to generate sufficient products to be observed by NMR.

Finally, the pH dependence of E233Q is consistent with such a role. The acidic limb, presumed to be due to the nucleophile D197, is perturbed very little, as might be expected. However, the basic limb, generally assumed to be due to the general acid catalyst, is altered substantially and appears to reflect at least two ionizations. These likely arise from other nearby ionizing side chains in the absence of the true acid catalyst.

Speculation Concerning the Role of D300. Since D197 and E233 appear to be the nucleophile and general acid catalyst, respectively, the question remains as to the role of D300, the third, highly conserved active site carboxyl group. The kinetic parameters for D300A and D300N demonstrate that D300 is a crucial residue in the catalytic mechanism. As with the other mutants, most of the reduction in the k_{cat}/K_m values (10^4-10^5-fold) is due to the reduction in k_{cat} values, since the K_m values are less than 3-fold higher than the values for the wild-type enzyme. The recent X-ray crystal structure of the family 13 enzyme CGTase trapped as its glycosyl-enzyme intermediate (*18*) has suggested that D300 aids in the deformation of the sugar bound to the −1 subsite from the ground-state chair conformation toward the transition-state half-chair conformation. In addition, D300 appears to play a role in enhancing the electrophilicity of the sugar anomeric carbon via a hydrogen-bonding interaction with the hydroxyl group at C2 (*18*). The reduction in k_{cat} with

the D300N mutant is, therefore, postulated to arise from altered hydrogen bonding in the −1 subsite as a result of the reduced ability of the amide to aid the nucleophilic attack during glycosylation. These functions, however, would be difficult to glean from simple kinetic studies.

CONCLUSIONS

The studies presented here represent a detailed mechanistic analysis of three active site carboxyl groups in human pancreatic α-amylase based on the combined use of site-directed mutagenesis and kinetic and structure determination techniques. The evidence obtained clearly supports the hypothesis that D197 plays the role of the catalytic nucleophile. Comparison of the kinetic parameters of "activated" versus "unactivated" substrates allowed us to conclude that E233 is the general acid catalyst. Additional kinetic studies and product distribution profiles provide clear evidence that D300 plays a significant role in catalysis by HPA; however, the precise nature of that role remains unclear.

ACKNOWLEDGMENT

We thank Mr. Shouming He for obtaining the mass spectra, Mr. Gary Sidhu for assistance with structural studies, Mr. Shin Numao for aid in manuscript preparation, and Dr. R. A. J. Warren for generous donation of the endoglycosidase F−CBD fusion protein.

REFERENCES

1. Henrissat, B. (1991) *Biochem. J. 280*, 309−316.
2. Henrissat, B., Callebaut, I., Fabrega, S., Lehn, P., Mornon, J. P., and Davies, G. (1995) *Proc. Natl. Acad. Sci. U.S.A. 92*, 7090−7094.
3. Henrissat, B., and Davies, G. (1997) *Curr. Opin. Struct. Biol. 7*, 637−644.
4. Braun, C., Meinke, A., Ziser, L., and Withers, S. G. (1993) *Anal. Biochem. 212*, 259−262.
5. MacGregor, E. A. (1988) *J. Protein Chem. 7*, 399−415.
6. Svensson, B., and Søgaard, M. (1993) *J. Biotechnol. 29*, 1−37.
7. Svensson, B. (1994) *Plant Mol. Biol. 25*, 141−157.
8. Qian, M., Haser, R., Buisson, G., Duee, E., and Payan, F. (1994) *Biochemistry 33*, 6284−6294.
9. Larson, S. B., Greenwood, A., Cascio, D., Day, J., and McPherson, A. (1994) *J. Mol. Biol. 235*, 1560−1584.
10. Machius, M., Wiegand, G., and Huber, R. (1995) *J. Mol. Biol. 246*, 545−559.
11. Suzuki, A., Yamane, T., Ito, Y., Nishio, T., Fujiwara, H., and Ashida, T. (1990) *J. Biochem. 108*, 379−381.
12. Brady, R. L., Brzozowski, A. M., Derewenda, Z. S., Dodson, E. J., and Dodson, G. G. (1991) *Acta Crystallogr. B47*, 527−535.
13. Swift, H. J., Brady, L., Derewenda, Z. S., Dodson, E. J., Dodson, G. G., Turkenburg, J. P., and Wilkinson, A. J. (1991) *Acta Crystallogr. B47*, 535−544.
14. Brayer, G. D., Luo, Y. G., and Withers, S. G. (1995) *Protein Sci. 4*, 1730−1742.
15. Kadziola, A., Abe, J., Svensson, B., and Haser, R. (1994) *J. Mol. Biol. 239*, 104.
16. Ramasubbu, N., Paloth, V., Luo, Y. G., Brayer, G. D., and Levine, M. J. (1996) *Acta Crystallogr., Sect. D: Biol. Crystallogr. D52*, 435−446.
17. Tao, B. Y., Reilly, P. J., and Robyt, J. F. (1989) *Biochim. Biophys. Acta 995*, 214−220.
18. Uitdehaag, J., Mosi, R., Kalk, K., van der Veen, B., Dijkhuizen, L., Withers, S., and Dijkstra, B. (1999) *Nat. Struct. Biol. 6*, 432−436.
19. Dauter, Z., Dauter, M., Brzozowski, A. M., Christensen, S., Borchert, T. V., Beier, L., Wilson, K. S., and Davies, G. J. (1999) *Biochemistry 38*, 8385−8392.
20. Kadziola, A., Sogaard, M., Svensson, B., and Haser, R. (1998) *J. Mol. Biol. 278*, 205−217.
21. Qian, M. X., Nahoum, V., Bonicel, J., Bischoff, H., Henrissat, B., and Payan, F. (2001) *Biochemistry 40*, 7700−7709.
22. Brayer, G. D., Sidhu, G., Maurus, R., Rydberg, E. H., Braun, C., Wang, Nguyen, N. T., Overall, C. M., and Withers, S. G. (2000) *Biochemistry 39*, 4778−4791.
23. Hayashi, M., Hashimoto, S., and Noyori, R. (1984) *Chem. Lett.*, 1747−1750.
24. Rydberg, E. H., Sidhu, G., Vo, H. C., Hewitt, J., Cote, H. C. C., Wang, Y., Numao, S., MacGillivray, R. T. A., Overall, C. M., Brayer, G. D., and Withers, S. G. (1999) *Protein Sci. 8*, 635−643.
25. Kunkel, T. A., Roberts, J. D., and Zakou, R. A. (1987) *Methods Enzymol. 154*, 367−382.
26. Sanger, F., Nicklen, S., and Coulson, A. R. (1977) *Proc. Natl. Acad. Sci. U.S.A. 74*, 5463.
27. Wung, J. L., and Gascoigne, N. R. J. (1996) *BioTechniques 21*, 808−812.
28. Otwinowski, Z., and Minor, W. (1997) *Methods Enzymol. 276*, 307−326.
29. Brünger, A. T. (1992) *X-PLOR: A system for X-ray crystallography and NMR*, Yale University Press, New Haven, CT.
30. Jones, T. A., Zhou, J.-Y., Cowan, S. W., and Kjeldgaard, M. (1991) *Acta Crystallogr. A47*, 110−119.
31. Luzzati, P. V. (1952) *Acta Crystallogr. 5*, 803−810.
32. Bernfeld, P. (1955) *Methods Enzymol. 1*, 149−158.
33. McCarter, J., Adam, M., Braun, C., Namchuk, M., Tull, D., and Withers, S. G. (1993) *Carbohydr. Res. 249*, 77−90.
34. Laroche, Y., Storme, V., Meutter, J. D., Messens, J., and Lauwereys, M. (1994) *Bio/Technology 12*, 1119−1124.
35. Okada, G., Genghof, D. S., and Hehre, E. J. (1979) *Carbohydr. Res. 71*, 287−298.
36. Zakowski, J. J., and Bruns, D. E. (1985) *Criti. Rev. Clin. Lab. Sci. 21*, 283−322.
37. Ishikawa, K., Matsui, I., Honda, K., and Nakatani, H. (1992) *Biochem. Biophys. Res. Commun. 183*, 286−291.
38. Ly, H. D., and Withers, S. G. (1999) *Annu. Rev. Biochem. 68*, 487−522.
39. Zechel, D. L., and Withers, S. G. (2000) *Acc. Chem. Res. 33*, 11−18.
40. Wang, Q., Trimbur, D., Warren, R. A. J., and Withers, S. G. (1995) *Biochemistry 34*, 14554−14562.
41. MacLeod, A. M., Tull, D., Rupitz, K., Warren, R. A. J., and Withers, S. G. (1996) *Biochemistry 35*, 13165−13172.
42. Lawson, S. L., Wakarchuk, W. W., and Withers, S. G. (1997) *Biochemistry 36*, 2257−2265.
43. Mosi, R., He, S. M., Uitdehaag, J., Dijkstra, B. W., and Withers, S. G. (1997) *Biochemistry 36*, 9927−9934.

BI011821Z